Quantum Detection of Binary and Ternary Signals in the Presence of Thermal Noise Fields

V. A. Vilnrotter[1] and C.-W. Lau[1]

A new technique for evaluating the performance of quantum signals observed in the presence of noise is described and evaluated. The quantum theory for detecting coherent-state signals has been developed previously; however, the quantum signal-plus-noise problem has received little attention due to its complexity. Here we develop a discrete approximation to the coherent-state representation of signal-plus-noise density operators, and present solutions to optimum receiver performance in terms of quantum measurement states whose performance is optimized via generalized rotations in Hilbert space. An efficient algorithm for carrying out the required numerical optimization is described and applied to binary signals observed in the presence of noise, for which exact results are available for comparison. The algorithm is then applied to the detection of ternary signals observed in the presence of noise, a previously unsolved problem, and the performance of the optimum receiver is characterized.

I. Introduction

The classical communications model assumes that deterministic signals are observed in the presence of additive Gaussian noise. This model is adequate for describing communications at radio frequencies, where quantum effects are not readily detectable. However, at optical frequencies, quantum effects become the dominant source of error and must be taken into account. An approach consistent with the principles of quantum mechanics starts by quantizing the received electromagnetic field and seeks to determine those measurements on the received field that achieve the best performance, such as minimizing the average probability of detection error. Exact solutions for the case of coherent states used in both binary and higher-dimensional signal sets have been described in the literature [1–4]. The quantum mechanical solution for pure-state signals (the noiseless case) can be formulated in terms of Kennedy's orthogonal measurement states, involving optimization of the detection operator over the signal

[1] Communications Systems and Research Section.

The research described in this publication was carried out by the Jet Propulsion Laboratory, California Institute of Technology, under a contract with the National Aeronautics and Space Administration.

subspace [2,3]. Recently, efficient algorithms have been developed to carry out the required optimization and applied to higher-dimensional signals of interest in optical communications, including pulse position modulation (PPM) and dense signal sets such as quadrature phase-shift keying (QPSK) and binary phase-shift-keyed PPM (BPSK-PPM), as described in [5,6].

The addition of thermal noise fields to the received coherent-state field complicates the problem significantly, and hence exact solutions to the quantum signal-plus-noise problems generally are not known. One class of problems that can be solved numerically is the class of binary coherent-state signals in the presence of thermal noise fields, where the solution involves finding the positive eigenvalues of the difference of density operators under the two hypotheses in matrix form [1,3]. However, for higher-dimensional signals, solutions are not readily available.

Here we present an approach that can be used to evaluate the performance of higher-dimensional signal sets observed in the presence of noise. The solution involves an approximation to the density operators, followed by detection in terms of optimized measurement states defined over the signal-plus-noise subspace. Detection operators, expressed in terms of orthogonal measurement states, first are applied to binary signals whose performance in the presence of noise is known, for purposes of evaluation and comparison. This approach then is applied to a three-signal ternary detection problem, and performance in the presence of noise is determined. Although currently only ternary signals are considered due to computational complexity, this technique can be extended to higher-dimensional signal sets, providing the capability to determine optimum performance in the presence of noise for a large class of signals.

II. Quantum Representation of Signal Plus Noise

A. Coherent-State Representation of Signals

Coherent states, representing electromagnetic radiation produced by physical devices such as lasers, are an important class of states for optical communications. It is well known [7] that the coherent states of a single mode of radiation $|\alpha\rangle$ can be expressed in the form of a superposition of orthonormal states $|n\rangle$, known as the number states:

$$|\alpha\rangle = e^{-(1/2)|\alpha|^2} \sum_{n=0}^{\infty} \frac{\alpha^n}{(n!)^{1/2}} |n\rangle \tag{1}$$

The coefficients of the number states are governed by the complex parameter α. Each number eigenstate $|n\rangle$ contains n photons, and hence the probability of obtaining exactly n photons as the outcome of an experiment can be computed as

$$|\langle \alpha | n \rangle|^2 = e^{-|\alpha|^2} \frac{|\alpha|^{2n}}{n!} \tag{2}$$

For any n, this expression specifies Poisson probabilities for the number of photons, with the average number of photons equal to $|\alpha|^2 \equiv N_s$. Coherent states are not orthogonal, as can be shown by considering the overlap between two arbitrary coherent states, $|\alpha_1\rangle$ and $|\alpha_2\rangle$. Orthogonality requires the overlap to vanish; however, for coherent states, the squared magnitude of the overlap is not zero but is given by the following expression:

$$|\langle\alpha_1|\alpha_2\rangle|^2 = \left| e^{-(|\alpha_1|^2+|\alpha_2|^2)/2} \sum_n \sum_m \frac{\alpha_1^n}{\sqrt{n!}} \frac{(\alpha_2^*)^m}{\sqrt{m!}} \langle n|m\rangle \right|^2 = \left| e^{-(|\alpha_1|^2+|\alpha_2|^2-2\alpha_1\alpha_2^*)/2} \right|^2 = e^{-|\alpha_1-\alpha_2|^2} \quad (3)$$

Equation (3) demonstrates that there is always some overlap between coherent states, regardless of how great the average photon count in each state may be.

B. Coherent-State Representation of Signal Plus Noise

The representation of coherent states as a superposition of number states is valid only when the receiver observes a pure-state signal with a known α parameter. Incorporation of the effects of classical randomness, such as a random α parameter or thermal noise fields entering the receiver along with the signal, requires the introduction of the density operator, ρ, defined in terms of an appropriate basis $\{|\varphi_k\rangle\}$ as

$$\rho = \sum_{k=0}^{\infty} P_k |\varphi_k\rangle\langle\varphi_k| \quad (4)$$

where $\sum_{k=0}^{\infty} P_k = 1$. For a pure coherent state, the density operator consists of a single term: $\rho = |\alpha\rangle\langle\alpha|$. The density operator for a coherent-state signal plus background radiation in a single mode of the received field can be represented in terms of a continuum of coherent states as [1]

$$\rho = (\pi N)^{-1} \int \exp(-|\alpha-\mu|^2/N)|\alpha\rangle\langle\alpha| d^2\alpha \quad (5)$$

where μ is the complex envelope of the coherent-state vector representing the signal in the absence of thermal noise and N is the average number of photons in a single mode of the noise field. In the plane of complex numbers, α, the Gaussian weight function is centered over the origin when there is no signal and shifted to the complex number μ when a signal is present, where $|\mu|^2$ denotes the average photon energy of the signal. An approximate discrete representation of Eq. (5) can be obtained by replacing the integral with an infinite sum, yielding

$$\tilde{\rho} \cong (\pi N)^{-1} \sum_{j=0}^{\infty} \sum_{k=0}^{\infty} \int_{A_{jk}} \exp(-|\alpha-\mu|^2/N)|\alpha_{jk}\rangle\langle\alpha_{jk}| d^2\alpha$$

$$= \sum_{j=0}^{\infty} \sum_{k=0}^{\infty} P_{jk} |\alpha_{jk}\rangle\langle\alpha_{jk}| \quad (6)$$

where $P_{jk} = (\pi N)^{-1} \int_{A_{jk}} \exp(-|\alpha-\mu|^2/N) d^2\alpha$, and $|\alpha_{jk}\rangle$ is the approximating discrete coherent state with complex parameter α_{jk} obeying the constraint $\sum_{j,k} P_{jk}|\alpha_{jk}|^2 = N$, where N is the average number of photons in a single mode and $\{A_{jk}\}$ are small disjoint areas covering the α-plane. We can interpret the sum in Eq. (6) as defining a countable set of coherent states, each occurring with probability defined by the integral of the Gaussian weight function over the area associated with the approximating coherent

state. The probability P_{jk} of receiving a coherent state within a specified small region of the α-plane, A_{jk}, is given by the integral of the weight function over that region. This model will be referred to as the discrete coherent-state, or DCS, approximation.

Since coherent states separated by a distance of one unit in the α-plane evaluate to 0.368 and decrease rapidly for greater distances, Eq. (3), this suggests approximating the continuous α-plane with discrete samples on a regular grid of points separated by one unit, for applications where relatively large regions of the α-plane are involved. In effect, this approximation collapses small neighborhoods onto a single coherent state located at a specific grid point and has the advantage of reducing the complexity of the representation. A graphical representation of the DCS approximation is shown in Fig. 1, illustrating an approximate density operator for thermal noise near the origin of the complex α-plane with adjacent coherent states separated by one unit. Since coherent states separated by one unit or more have a relatively small overlap, this model is expected to yield accurate results for cases where the Gaussian weight function is broad enough to have significant probability at a radius of one unit or more from the center of the weight function, and will be used as the starting point for evaluating detection performance.

The notation for labeling the coherent-state centers in Fig. 1 anticipates the application of this model to detection, where the absence of signal energy generally is referred to as the null hypothesis, or H_0: a cluster of coherent states around the origin represents the density operator for noise only, or H_0, hence the common zero in the subscripts signifying the null hypothesis.

Adopting the numbering scheme of Fig. 1, according to which coherent states far from the center μ are assigned increasingly higher values, and further noting that, for a Gaussian weight distribution, coherent states with an α-parameter far from the center are not very likely to occur, the infinite limits in Eq. (6) can be replaced by finite limits as a further approximation. This finite representation of the density operator will be used in the rest of this article to evaluate detection performance of the quantum receiver for various modulation schemes in the presence of noise.

C. Quantum Detection in the Presence of Noise

The DCS noise model is first applied to binary on–off keying (OOK) signals. Under hypothesis zero, denoted by H_0, only thermal noise is received, whereas under hypothesis one, H_1, a coherent-state signal

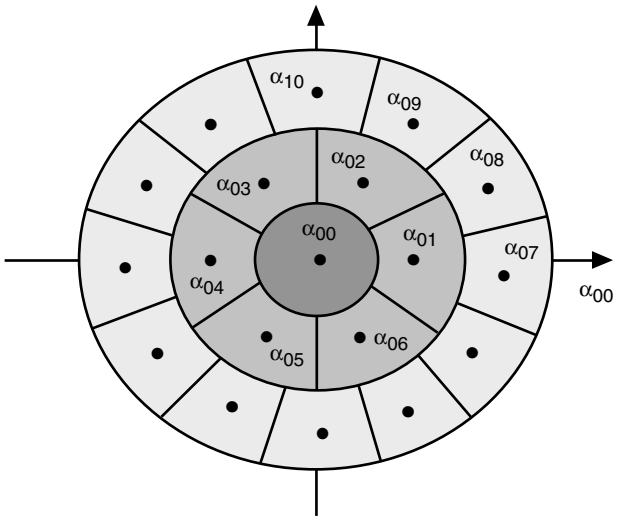

Fig. 1. Discrete coherent-state (DCS) representation of the density operator for zero-mean noise.

plus thermal noise enters the receiver. Using the approximation in Eq. (6), and renaming the subscripts to reflect the hypotheses as shown in Fig. 1, the following approximate density operators are obtained:

$$\left.\begin{aligned} H_0: \quad & \tilde{\rho}_0 = \sum_{k=0}^{K} P_{0k} |\alpha_{0k}\rangle\langle\alpha_{0k}| \\ H_1: \quad & \tilde{\rho}_1 = \sum_{k=0}^{K} P_{1k} |\alpha_{1k}\rangle\langle\alpha_{1k}| \end{aligned}\right\} \tag{7}$$

These density operators define the probability of occurrence of coherent states approximating the noise distribution, with coherent state $|\alpha_{0k}\rangle$ occurring with probability P_{0k} under H_0, and $|\alpha_{1k}\rangle$ with probability P_{1k} under H_1. This formulation leads to an approximate model according to which any one of a large number of coherent states could occur under either hypothesis due to the presence of noise.

Optimal detection of quantum states can be formulated in terms of projections onto orthonormal measurement states as described in [2–6]. In our model, the detection operator for the binary signal-plus-noise problem spans the entire signal-plus-noise subspace of Hilbert space. It is denoted by W_2, with components the projection operators Π_0 and Π_1, corresponding to the two hypotheses, H_0 and H_1:

$$W_2 = \Pi_0 + \Pi_1 \tag{8a}$$

$$\Pi_0 = \sum_{j=0}^{K-1} |w_{0j}\rangle\langle w_{0j}|; \quad \Pi_1 = \sum_{j=0}^{K-1} |w_{1j}\rangle\langle w_{1j}| \tag{8b}$$

The detection operator W_2 is a "resolution of the identity" defined over the signal-plus-noise subspace of the original Hilbert space spanned by the DCS representation of the density operators. The measurement-state components of these operators are orthonormal quantum states of the form $|w_{00}\rangle, \cdots, |w_{0(K-1)}\rangle$ and $|w_{10}\rangle, \cdots, |w_{1(K-1)}\rangle$, respectively. These detection operators are projectors; hence, their eigenvalues are either zero or one [1]. Application of the detection operator W_2 to the received coherent state plus noise results in the received coherent state projecting onto one of the measurement states as the outcome of the measurement. If the outcome of the measurement is the projection of the received coherent state onto an eigenstate of Π_0, then H_0 is selected; otherwise the receiver decides that H_1 was transmitted. Note that every noise-corrupted signal state is represented by exactly K discrete coherent states; hence, $2K$ measurement states are needed for optimum detection of binary signals in the presence of noise.

Detection operators for the general M-hypothesis problem can be formulated in a similar manner. Now there are M density operators, denoted by $\rho_0, \rho_1, \cdots, \rho_{M-1}$, and the detection operator for the M-hypothesis problem, W_M, is of the form

$$W_M = \sum_{m=0}^{M-1} \Pi_m \tag{9a}$$

$$\Pi_m = \sum_{j=0}^{K-1} |w_{mj}\rangle\langle w_{mj}| \tag{9b}$$

The detection operators correspond to a receiver structure whose performance can be determined using numerical techniques. The detection operator W_M is simultaneously applied to the entire signal-plus-noise subspace, encompassing all hypotheses and the effects of noise. The probability of correct detection is found by first determining the expected values of the component projection operators, and then averaging over all hypotheses. For example, given H_0, the probability of projecting onto one of the eigenvectors of Π_0 is equal to the expected value of Π_0:

$$
\begin{aligned}
P[C|H_0] = E(\Pi_0) &= \sum_{j=0}^{K-1} \langle w_{0j}|\tilde{\rho}_0 \Pi_0 |w_{0j}\rangle \\
&= \sum_{j=0}^{K-1} \langle w_{0j}| \sum_{l=0}^{K-1} P_{0l}|\alpha_{0l}\rangle\langle\alpha_{0l}| \sum_{m=0}^{K-1} |w_{0m}\rangle\langle w_{0m}|w_{0j}\rangle \\
&= \sum_{j=0}^{K-1}\sum_{l=0}^{K-1} P_{0l}\langle w_{0j}|\alpha_{0l}\rangle\langle\alpha_{0l}|w_{0j}\rangle \\
&= \sum_{j=0}^{K-1}\sum_{l=0}^{K-1} P_{0l}|\langle w_{0j}|\alpha_{0l}\rangle|^2 \qquad (10)
\end{aligned}
$$

The probability of correct detection is obtained by averaging the conditional probabilities for each hypothesis: $P(C) = \sum_m P(H_m)P[C|H_m]$, where $P(H_m)$ are the a priori probabilities. The average probability of error follows as $P(E) = 1 - P(C)$.

It is interesting to compare the receiver for the DCS model developed here to the quantum receiver that is optimum for the pure-state (noiseless) case. In the pure-state formulation, there is only one measurement state associated with each hypothesis; hence, correct detection occurs if the received coherent state projects onto the single measurement state associated with it. If only two measurement states were used to detect signal-plus-noise states as defined by the DCS model, then correct detection would occur if any of the coherent states in a cluster of K coherent states projected onto the single measurement state associated with that hypothesis. However, with the detection operators described above, not one but K measurement states are associated with each hypothesis, and projection of the received coherent state onto any of the K measurement states associated with that hypothesis results in correct detection. By contrast, the conditional probability of correct detection in the DCS formulation contains K^2 positive terms, since now there are K measurement states, and all possible projections onto every measurement state are included in the sum, as shown in Eq. (10), resulting in greater conditional probability of correct detection.

The conditional probability for pure-state detection is given by the expression

$$
P(C|H_0) = \sum_{l=0}^{K-1} |\langle w_0|\alpha_{0l}\rangle|^2 \qquad (11)
$$

demonstrating that the conditional probability contains only K terms when the receiver designed for only two coherent states is applied to the DCS model.

The detection operators described above span the relevant signal-plus-noise subspace but were chosen arbitrarily; hence, they do not minimize the average probability of error. Best performance is obtained when the measurement states are optimized so as to maximize the average probability of correct detection. Since the detection operators consist of rigid orthogonal measurement states, the required optimization can be formulated in terms of rotations of the detection operators in Hilbert space. The details of the numerical optimization via rigid rotations of the detection operators are the subject of the following section.

III. Optimization of the Detection Operators

Numerical optimization of the detection operators consists of finding the orientation of the orthogonal measurement states that yield the maximum probability of correct detection or, equivalently, the minimum probability of error. As shown in previous articles [5,6], the solution to the general M-hypotheses problem can be found by rotating the measurement states in an M-dimensional Hilbert space, and calculating the probability of correct detection for each rotation until the global maximum is found. To summarize the original approach, the optimization problem can be solved iteratively starting with two dimensions, since it is possible to rotate the projections of a vector in any lower dimension without affecting the projections of that vector onto the higher dimensions. For example, this principle is illustrated in Fig. 2, where the projection of an arbitrary vector V_1 in the x–y plane is given by $V_1 \cos(\psi)$. The vector V_1 can be rotated such that the projection onto the z-axis is unchanged while the x- and y-projection components vary. Generalizing this result to any arbitrary N-dimensional vector, the projections onto $(N-1)$ coordinate axes can be varied by rotating each of the $(N-1)$ measurement coordinates without affecting the projection onto the next higher dimension. Given M hypotheses and K states per hypothesis, a total of $N = MK$ dimensions is required for optimization.

The application of these principles to measurement states is straightforward since measurement states are orthogonal and can be thought of as analogous to axes in an arbitrary Hilbert space. Making use of this dimensional independence, the measurement states are incrementally rotated and the error probability calculated until the angle yielding the minimum probability of error is found for each dimension. To further simplify the search, each dimension only requires a rotation in a single plane. This plane is defined by the Nth dimensional axis and the $N-1$ dimensional bisector. The optimum measurement-state orientation for each dimension can be determined from the lower-dimensional solution, and this procedure is continued until the complete N-dimensional solution is obtained. However, when the signal

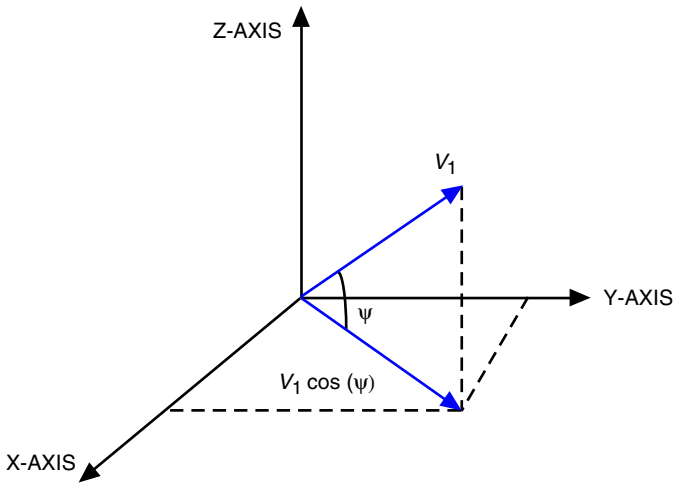

Fig. 2. Vector rotation.

states are not symmetrically placed, such as the case for OOK or BPSK in the presence of noise, the described diagonal rotation algorithm does not provide the true optimal orientation of the measurement states. In order to find the optimal orientation, the diagonal rotational algorithm described above must be extended.

The original rotation algorithm described above, and documented in [6], must be modified to accommodate the optimization for the non-symmetrical case. The measurement state orientation and probability of error solved for the symmetric case are used as an initial condition. The measurement axes then are incrementally rotated about each axis pair in the lower-dimensional space from 0 to 360 degrees. With each rotational increment, the angle of rotation and probability of error for the new orientation is measured. The new measurement-state orientation is accepted only if the probability of error is lower than that before. This operation is carried out for both directions, clockwise and counterclockwise.

Examples of the DCS representation for binary and ternary signals plus noise are shown in Fig. 3. In Fig. 3(a), OOK signal states are augmented with 4 additional coherent states to account for the effects of noise, so that $K = 5$. Each cluster representing a noise-corrupted signal in the DCS model, therefore, contains 5 coherent states, as depicted in Fig. 3(a). Figure 3(b) illustrates the DCS representation of BPSK signals with noise, $K = 7$. Figure 3(c) is an example of ternary signals with $K = 5$.

For the binary DCS problem, this yields a total of 10 coherent states, $|\alpha_{0i}\rangle$ and $|\alpha_{1i}\rangle$, $i = 0, 1, 2, 3, 4$. Correspondingly, there will be a total of 10 measurement states $|w_{0i}\rangle$ and $|w_{1i}\rangle$, $i = 0, 1, 2, 3, 4$. In order to provide an approximation to the sampling scheme described earlier, a two-circle scheme was adopted for the probability distribution. The probability for the primary coherent state representing the signal, in the small circle in Fig. 3(a), was computed using a radius of $r = 0.5$ units. The 4 coherent states surrounding the primary coherent state were located at a radius of 1.0 unit from the center. The radius of the large circle was set at $r = 1.5$ units. The probability distribution for each

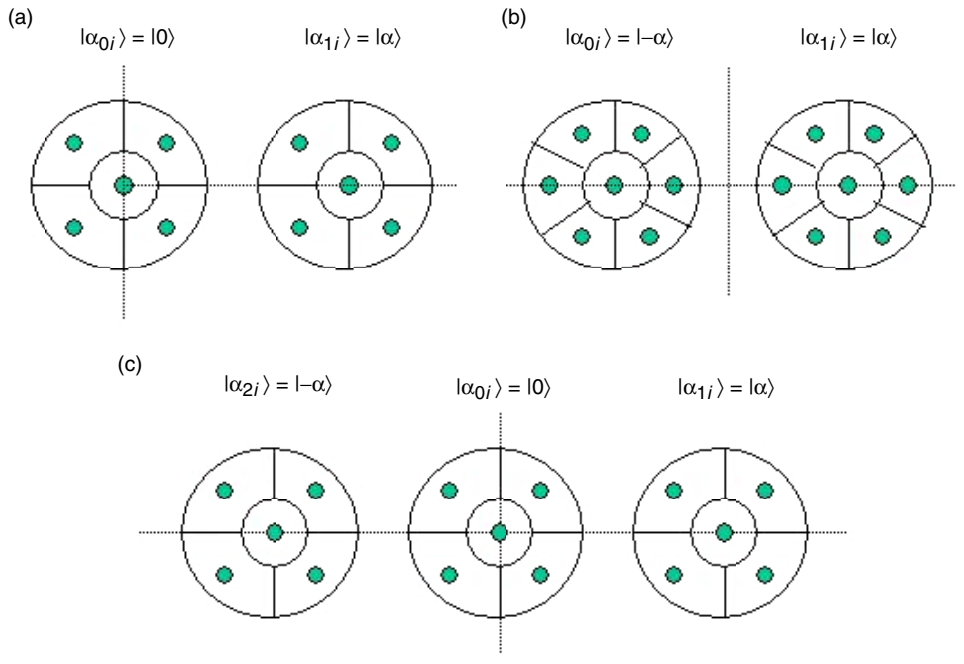

Fig. 3. Placement of the approximating coherent states in the DCS representation, and the sectors used to calculate probabilities of occurrence: (a) 10 dimensions: OOK signals, (b) 14 dimensions: BPSK signals, and (c) 15 dimensions: ternary signals.

state then was computed as follows. The probability of occurrence of the coherent states under H_0 is governed by the density operator

$$\hat{\rho}_0 \cong (\pi N)^{-1} \sum_{k=0}^{K} \int_{A_{0k}} e^{-|\alpha_{0k}|^2/N} |\alpha_{0k}\rangle\langle\alpha_{0k}| d^2\alpha \tag{12}$$

Integrating the weight function over a circle of radius r yields the equation

$$P(r) = 1 - e^{-(r^2/N)} \tag{13}$$

which can be used to determine the probabilities associated with each coherent state in the cluster by evaluating the probabilities $P_{jk} = (\pi N)^{-1} \int_{A_{jk}} \exp(-|\alpha - \mu|^2/N) d^2\alpha$ over the appropriate regions. For example, with $K = 5$ and inner circle radius $r = 0.5$, $P_{00} = 1 - e^{-0.25/N}$, whereas the probabilities associated with the outer circle with radius $r = 1.5$ are $P_{0k} = (1/4)(1 - e^{-2.25/N} - P_{00}$; $k = 1, 2, 3, 4$.

This serves as the initial starting point for the second optimization algorithm. The measurement states are incrementally rotated about each higher-dimensional axis pair in the signal set from 0 to 360 degrees. For each incremental rotation, the probability of error is calculated using Eq. (10). Using the 10-dimensional setup as an example, the algorithm begins by rotating the measurement states in the x–y plane from 0 to 360 degrees. The angle yielding the minimum probability of error is determined, and the orientation of the measurement states is set at the minimum angle. The new measurement-state orientation then is rotated in the x–y plane, the minimum probability of error is determined, and the measurement-state orientation is reset accordingly. This rotation process is repeated until all axis pairs have been rotated. The process then is repeated with rotation in the negative direction from 0 to −360 degrees. After all the rotations have been completed, a minimum probability of error will be found that corresponds to the optimal orientation of the measurement states. This approach can be generalized up to N dimensions by systematically rotating about each axis pair and finding the minimum probability of error.

IV. Numerical Results

Performance of the optimized detection operators for the DCS noise model have been evaluated, using the state–space optimization technique described above. The results for OOK and BPSK signals using both 5-dimensional and 7-dimensional clusters in the DCS model ($K = 5$ and $K = 7$) are shown in Figs. 4 and 5, representing probability of error as a function of the average number of signal photons, $N_s = |\mu|^2$. In both figures, dashed curves refer to the results for $K = 5$ and solid curves for $K = 7$. The exact error probabilities obtained previously via the eigenvalue method are labeled "Q-Opt" in both figures. Comparisons of optimum quantum detection of binary signals with classical detection techniques such as photon counting and coherent detection are treated elsewhere [1,4,5], where it is shown that classical detection techniques are often 3 dB worse than optimum quantum detection.

With OOK signaling, the received signal field is in a coherent state $|\alpha\rangle$ under hypothesis one, and in state $|0\rangle$ under hypothesis zero, as shown in Fig. 3(a). Thermal noise entering the receiver along with the signal generates the approximate density operators defined in Eq. (6). The performance of the optimum quantum detector for OOK signals in the absence of noise has been evaluated previously using measurement-state techniques and documented in [4]. The approximate error probabilities obtained with the DCS technique are compared with the known performance of the optimum quantum detector, obtained by evaluating the eigenvalues of the difference of the density operators under the two hypotheses [1,3].

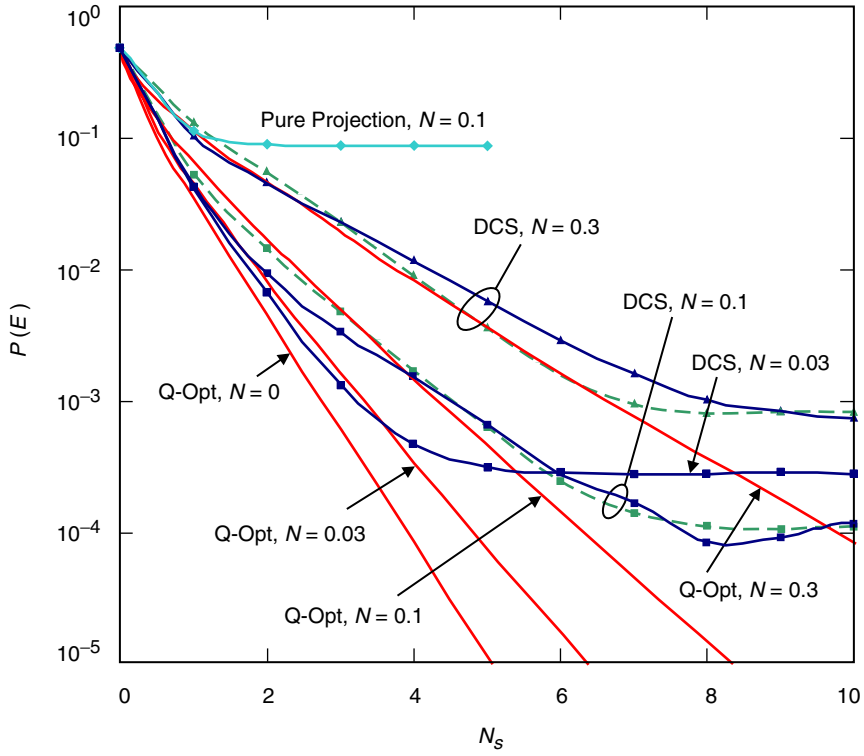

Fig. 4. Performance of the approximate DCS algorithm and optimum quantum detector for binary OOK signals in the presence of noise: $K = 5$ and 7.

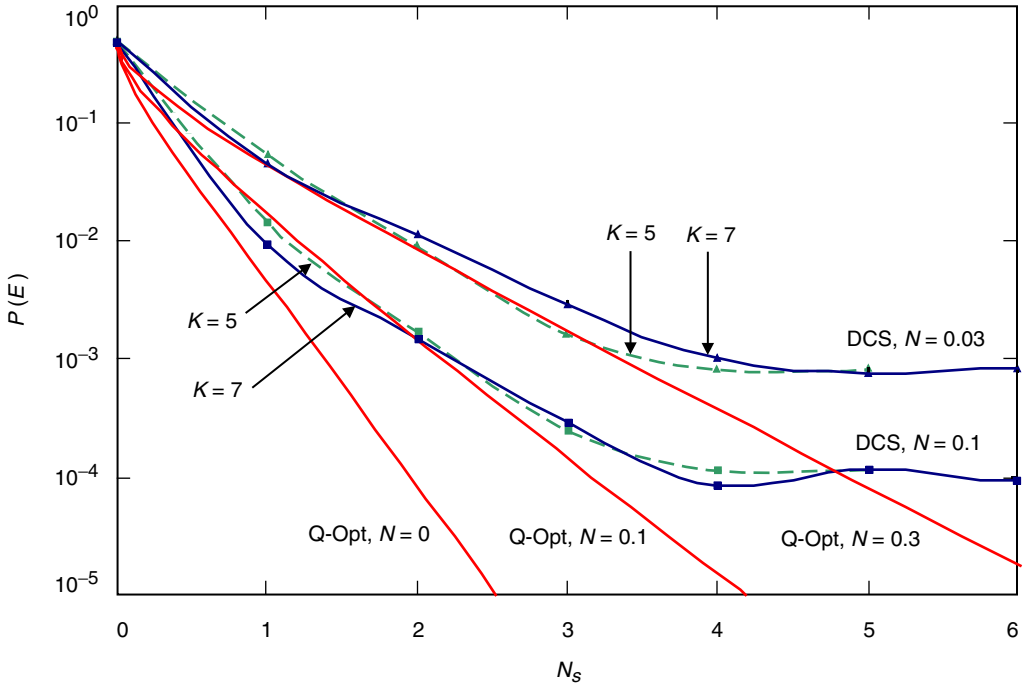

Fig. 5. Performance of the approximate DCS algorithm with BPSK signals compared to known solutions for optimum quantum detection in the presence of noise: $K = 5$ and 7.

As expected, even small amounts of thermal radiation degrade optimum receiver performance significantly: an average noise count of 0.1 photons per symbol degrades performance by more than 2 dB, whereas higher levels of noise corresponding to 0.3 photons per symbol lead to over 4-dB performance degradation.

The DCS technique with five coherent states separated by one unit was found to yield accurate error probabilities for values that exceed the small probability mass remaining outside the largest approximating ring. These probabilities can be found using Eq. (13): for the higher noise case of $N = 0.3$, the probability outside the first ring is 6×10^{-4}. It is clear from Fig. 4 that this value is consistent with the floor of the DCS error probability. It was found that other ad hoc approximations, such as assigning all of the probability outside the first ring to the coherent states in the second ring, usually resulted in worse performance; one reason could be that these ad hoc probability assignments fail to approximate the Gaussian distribution adequately.

When seven coherent states were used, $K = 7$, the areas were equalized by increasing the radius of the central region slightly so as to equal the area of each region on the first ring. Therefore, the probability assigned to the central coherent state was slightly greater, which could account for the apparent "better than optimum" performance exhibited at lower signal energies, particularly for the intermediate noise case of $N = 0.1$. However, other effects, such as algorithm error due to insufficient rotation resolution also could be the cause, as could less than optimum sampling of the α-plane. A complete understanding of the detailed behavior of the DCS approximation and the rotation algorithm will require further investigation.

For the lower noise cases, $N = 0.1$ and $N = 0.03$, the floor is due primarily to numerical errors resulting from the 1-degree rotation increments used in the algorithm. This was verified by recomputing a few points with 0.1-degree increments, which resulted in an order of magnitude reduction in the noise floor. Therefore, lower error probabilities can be reached with the optimized rotation algorithm by using smaller increments, but at the expanse of computation time. For the low-noise case of $N = 0.03$, the coherent states were placed closer together, separated by only 0.75 unit, because the Gaussian distribution for this case is so narrow that there is no appreciable probability outside the central region ($P_{0k} \simeq 4 \times 10^{-5}$ for the case $K = 7$ and separation of 1 unit).

The performance of the pure projection detection operator that is optimum for the noiseless case also has been evaluated. Note that for moderate modal noise counts corresponding to $N = 0.1$, the probability of bit error for the pure projection algorithm reaches a floor at an error probability of approximately 0.1 over the range considered, whereas the DCS algorithm continues to track the optimum solution until the much lower limiting value of approximately 10^{-4} is reached, as shown in Fig. 4.

Error probabilities for BPSK signals using both 5- and 7-dimensional DCS noise models are shown in Fig. 5 and compared to the optimum quantum detector as a function of the average number of photons per symbol. For this modulation format, the state of the received field in the absence of noise is denoted by $|\alpha\rangle$ under hypothesis one, and by $|-\alpha\rangle$ under hypothesis zero. Although the procedure for optimizing the measurement-state detection operators is identical to the OOK case, classical detection of these modulation formats is completely different. Since OOK represents an intensity modulation, it can be detected using direct detection techniques such as photon counting; however, BPSK is a phase-modulated format and, therefore, requires coherent detection techniques. It is again evident that the DCS approximation yields accurate results for error probabilities that exceed the uncounted probability outside the first DCS ring. Note that BPSK signals require only about half the average signal photons per symbol to reach a given error probability as compared with OOK signaling. However, since BPSK signals transmit a signal pulse under both hypotheses, whereas OOK transmits a signal only under the signal hypothesis and nothing under the alternative, BPSK modulation actually requires twice as many photons per symbol, on the average, as does OOK modulation. When compared on the basis of average transmitted power, both modulation schemes exhibit similar performance.

Finally, the DCS algorithm was applied to the problem of estimating the performance of the optimum quantum receiver for ternary signals in the presence of noise. An example of this signaling scheme is the three signal states $|\alpha\rangle$, $|-\alpha\rangle$, and $|0\rangle$. The DCS noise model now consists of three clusters in the α-plane, placed as shown in Fig. 3(c). The DCS algorithm places 15 measurement states near the discrete coherent states in such a way as to maximize the probability of correct detection. Application of the DCS algorithm yields the symbol-error probabilities $P(SE)$ for weak-noise ($N = 0.03$), moderate-noise ($N = 0.1$), and strong-noise ($N = 0.3$) cases shown in Fig. 6. For the strong-noise case, an error floor is reached at about 10^{-3}, again due to the probability mass ignored outside the second ring in the DCS model. For the low-noise cases, the error floor is dominated by the rotation increments in the optimization algorithm. Since the current limit of the optimization algorithm is 15 dimensions, clusters of 5 coherent states were used for each hypothesis ($K = 5$). Direct comparison with other results was not possible, however, since no previous solution to this problem could be found. The extension to higher-dimensional signal sets is conceptually straightforward using the DCS technique described here, but it requires extending the optimization algorithm to still higher dimensions.

V. Conclusions

A new technique has been developed to evaluate the performance of the optimum quantum receiver for coherent state signals in the presence of thermal noise. The continuous density operators for signal plus noise in the coherent-state representation were approximated by discrete operators. Detection operators for the discrete coherent states were defined in terms of orthogonal measurement states, and the probability of error was minimized by rotating the detection operators in Hilbert space. Optimum performance of the new DCS algorithm was verified using binary modulation formats whose performance in the presence of noise is well known [1,3]. The DCS algorithm then was applied to ternary modulation, whose performance in the presence of noise was not known previously, and performance curves under various noise conditions were obtained. This technique shows great promise for determining the performance of optimum quantum detectors for higher-dimensional signals in the presence of noise, such as pulse-position-modulated product-state signals and dense signal sets [5] contemplated for free-space communications, where no alternative methods for evaluating quantum receiver performance are available.

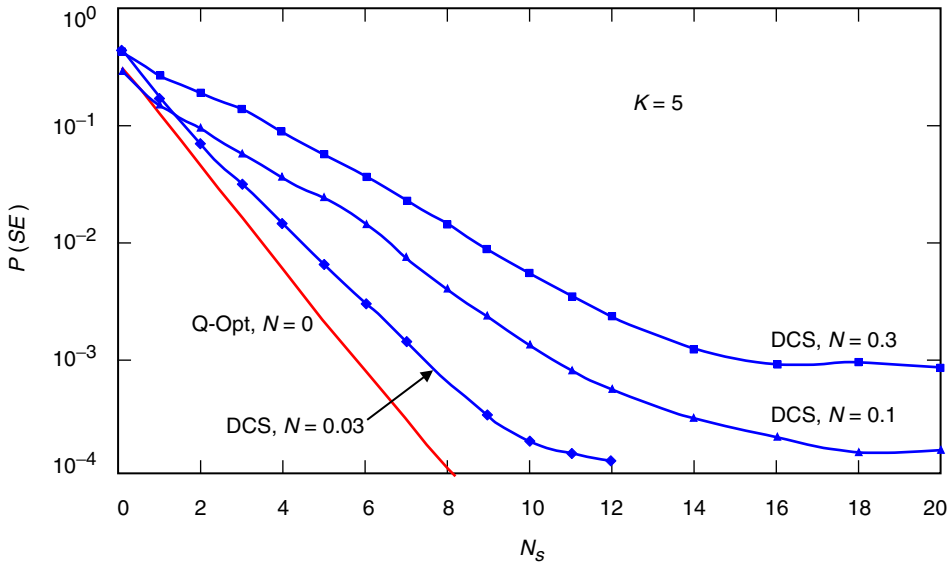

Fig. 6. Performance of the optimum quantum detection for ternary signals in the presence of noise: $K = 5$.

References

[1] C. W. Helstrom, J. W. S. Liu, and J. P. Gordon, "Quantum Mechanical Communications Theory," *Proceedings of the IEEE,* vol. 58, no. 10, pp. 1578–1598, October 1970.

[2] H. P. Yuen, R. S. Kennedy, and M. Lax, "Optimum Testing of Multiple Hypotheses in Quantum Detection Theory," *IEEE Transactions on Information Theory,* vol. IT-21, no. 2, pp. 125–134, March 1975.

[3] C. W. Helstrom, *Quantum Detection and Estimation Theory, Mathematics in Science and Engineering,* vol. 123, New York: Academic Press, 1976.

[4] V. Vilnrotter and C.-W. Lau, "Quantum Detection Theory for the Free-Space Channel," *The InterPlanetary Network Progress Report 42-146, April–June 2001*, Jet Propulsion Laboratory, Pasadena, California, pp. 1–34, August 15, 2001.
http://ipnpr.jpl.nasa.gov/tmo/progress_report/42-146/146B.pdf

[5] V. A. Vilnrotter and C.-W. Lau, "Quantum Detection and Channel Capacity for Communications Applications," *Proceedings of SPIE,* Free-Space Laser Communications Technologies XIV, San Jose, California, pp. 103–115, January 21–22, 2002.

[6] C.-W. Lau and V. A. Vilnrotter, "Quantum Detection and Channel Capacity Using State–Space Optimization," *The Interplanetary Network Progress Report 42-148, October–December 2001*, Jet Propulsion Laboratory, Pasadena, California, pp. 1–16, February 15, 2002.
http://ipnpr.jpl.nasa.gov/tmo/progress_report/42-148/148G.pdf

[7] R. J. Glauber, "Coherent and Incoherent States of the Radiation Field," *The Physical Review,* vol. 131, no. 6, pp. 2766–2788, September 15, 1963.